Published in final edited form as:
Conf Proc IEEE Eng Med Biol Soc. 2011 ; 2011: 1693–1696. doi:10.1109/IEMBS.2011.6090486.

Electrophysiological Models for the Heterogeneous Canine Atria: Computational Platform for Studying Rapid Atrial Arrhythmias

Oleg V. Aslanidi,
School of Physics and Astronomy, University of Manchester, Manchester M13 9PL, United Kingdom (tel: +44-161-275-3966; oleg.aslanidi@manchester.ac.uk).

Timothy D. Butters,
School of Physics and Astronomy, University of Manchester, Manchester M13 9PL, United Kingdom (timothy.butters@postgrad.manchester.ac.uk).

Christopher X. Ren,
School of Physics and Astronomy, University of Manchester, Manchester M13 9PL, United Kingdom (christopher.x.ren@student.manchester.ac.uk).

Gareth Ryecroft, and
School of Physics and Astronomy, University of Manchester, Manchester M13 9PL, United Kingdom (gareth.ryecroft@student.manchester.ac.uk).

Henggui Zhang
School of Physics and Astronomy, University of Manchester, Manchester M13 9PL, United Kingdom (henggui.zhang@manchester.ac.uk).

Abstract

Heterogeneity in the electrical action potential (AP) properties can provide a substrate for atrial arrhythmias, especially at rapid pacing rates. In order to quantify such substrates, we develop a family of detailed AP models for canine atrial cells. An existing model for the canine right atrial (RA) myocyte was modified based on electrophysiological data from dog to create new models for the canine left atrium (LA), the interatrial Bachmann's bundle (BB), and the pulmonary vein (PV). The heterogeneous AP models were incorporated into a tissue strand model to simulate the AP propagation, and used to quantify conditions for conduction abnormalities (primarily, conduction block at rapid pacing rated) in the canine atria.

I. Introduction

RAPID atrial arrhythmias, such as atrial fibrillation (AF), are considered to be a major cause of morbidity: they can cause reduction in cardiac output, a predisposition to stroke, heart failure and ventricular fibrillation, and hence, increased death rates [1-3]. Experimental animal studies and results of clinical endocardial mapping have suggested that AF may be sustained by re-entrant wavelets [4-6]. Precise mechanisms of such re-entry initiation remain unclear, but it is believed that atrial tissues with large regional differences in electrical properties are more susceptible to re-entry [5]. The latter may result from the conduction slowing and block in atrial tissue regions with longer refractoriness [7].

Animal cell and tissue experiments indicate that both atria are characterized by significant regional differences in the action potential (AP) morphology and duration, which are due to underlying variations in ionic channel currents [8-10]. However, relationships between the

Europe PMC Funders Author Manuscripts

ionic channel and AP heterogeneities and the resultant conduction abnormalities in the atria are difficult to dissect experimentally.

Computational modelling provides a framework for integrating such heterogeneous data and understanding the resultant arrhythmogenic behaviour [10-12]. Given the lack of data on the ionic heterogeneity in human atria, animal models offer the most sensible route to such a computational study. Despite availability of electrophysiological data [13], smaller rabbit atria cannot normally sustain AF [14]. Dog, the species most widely used in experimental AF studies [5], provides an extensive variety of data on atrial heterogeneity [7-10, 15]. Therefore, canine models can help provide novel insights into translational mechanisms of atrial arrhythmias.

The aim of this paper is to develop and study a family of canine models accounting for the ionic and AP heterogeneity between the right (RA) and left (LA) atria, the Bachmann's bundle (BB) and pulmonary veins (PV). An existing model for a canine RA myocyte [10] is modified based on available electrophysiological ionic channel and AP data [8-10, 15]. The resultant single cell AP models are incorporated into an atrial tissue model to study the AP conduction and quantify the relationships between the electrical heterogeneity and conduction abnormalities in the canine atria.

II. Methods

A. Model Development

The dynamics of electrical excitation in atrial tissues can be described by the following well-known equation [10-13]:

$$\frac{\partial V}{\partial t} = \nabla \cdot \mathrm{D} \nabla V - \frac{I_{\mathrm{ion}}}{C_m}. \quad (1)$$

Here V (mV) is the membrane voltage, ∇ is a spatial gradient operator, t is time (s), D is a diffusion coefficient (mm^2 ms^{-1}) that characterizes electrotonic spread of voltage via gap junctional coupling, I_{ion} is the total membrane ionic current (pA), and C_{m} (pF) is the membrane capacitance.

A biophysically detailed model describing individual ionic channel currents (such as I_{Na}, I_{CaL}, I_{to}, I_{Kr}, I_{Ks}, I_{K1}) comprising I_{ion} has been developed for a canine RA cell [10]. The model accurately reproduces the voltage-clamp data on which it has been based, and provides feasible morphologies for the AP in several distinctive types of RA cells. However, the model [10] does not account for heterogeneities between (i) RA and LA cells, (ii) both atria and the interatrial connection via BB, and (iii) LA and myocardial sleeves of the PV. All these heterogeneities are believed to play important roles in atrial arrhythmogenesis [15-17, 19-21] (see Discussion below).

We develop a new family of models for the canine LA, PV and BB cells based on the published electrophysiological voltage clamp and AP data [8-10, 15]. In cases when canine data is limited (e.g., the BB), we used well-documented data from rabbit [13]; using cross-species data is an accepted practice in cardiac modelling in situations where complete data from a single species are not available [11, 18].

Eq. (1) is used to simulate AP propagation in respective 1D atrial tissues. The diffusion coefficient is set to the value D = 0.2 mm^2 ms^{-1}, which produces the AP conduction velocity of ~0.65 m/s, as seen in experiments [17]. Eq. (1) is solved using the explicit Euler's method with time and space steps $\Delta t = 0.005$ ms and $\Delta x = 0.2$ mm, respectively.

B. Atrial Heterogeneities

Fig. 1 shows electrophysiological differences between the LA and RA observed experimentally in canine atria [8]. Recordings from canine atrial cells have shown insignificant differences in the current densities of I_{CaL}, I_{Ks}, I_{K1} and I_{to} between the LA and RA; the only significant difference in the ionic channel properties between the two atria is in the current density of the rapid delayed rectifier current, I_{Kr} [8]. Therefore, the conductance of I_{Kr} in the RA cell model [10] was increased to reproduce the higher current density in the LA cells (Fig. 1), as observed experimentally [8]. The AP morphology produced by the resultant LA cell model (Fig. 1) was also in agreement with experimental data from dog [8].

Fig. 2 shows heterogeneity between the RA and BB cells. Experimental data from rabbit [13] shows large differences in the ionic channel current densities of I_{CaL} and I_{K1}, as well as small differences in the current density of I_{to}, between the RA and BB cells (Fig. 2). As a result, the AP in the BB cells is significantly longer than that in RA cells (Fig. 2), as seen experimentally in rabbit [13] and dog [15]. Although the underlying ionic channel heterogeneity in dog has not been measured, it is not unreasonable to suggest that such heterogeneity is similar between the canine and rabbit cells.

Therefore, conductances of I_{CaL}, I_{K1} and I_{to} the canine RA cell model [10] were adjusted to qualitatively reproduce the experimentally observed differences in the current densities [13] and AP morphologies [15] between the RA and BB cells. Primarily, the conductance of I_{CaL} was increased, and the conductance of I_{K1} was decreased in the RA cell model, which resulted in a higher current density I_{CaL} and a lower current density of I_{K1} in the resultant BB cell model (Fig. 2). Combination of these significant changes in I_{CaL} and I_{K1} and a small decrease of I_{to} in the BB cell model (as compared to RA) resulted in the AP morphology which was in a good agreement with the experimental recordings from dog [15].

Fig. 3 shows heterogeneity between the LA and PV cells observed in experiments from canine atria [9]. Primarily, significant differences in the current densities of I_{CaL}, I_{Ks}, I_{K1} and I_{to} between the LA and PV cells result in different AP morphologies between these two cell-types. Therefore, we adjusted conductances of I_{CaL}, I_{Ks}, I_{K1} and I_{to} in the canine LA cell model to reproduce the differences in ionic channel current densities [9] between the LA and PV cells (Fig. 3); the AP morphology produced by the resultant PV model was also in agreement with experimental data from dog [9].

III. RESULTS

A developed family of AP models for the canine RA, BB, LA and PV cells can be incorporated into heterogeneous atrial tissue models to study the unknown mechanisms of AP conduction abnormalities in the atria. Note that such abnormalities are often seen experimentally [15-17, 19-20].

The developed 1D atrial tissue strand model (see in Fig. 4) was stimulated periodically at the varying basic cycle length (BCL), which resulted in the AP conduction from the RA region into the BB (Fig. 4). Stimulation at the physiological BCL of 600 ms resulted in continuous AP conduction through the strand: the AP conduction velocity in both the RA and BB regions had a uniform value of ~0.65 m/s. However, as the BCL was decreased to 220 ms, the AP conduction pattern became discontinuous (Fig. 4): the AP conduction velocity in the RA regions decreased to ~0.62 m/s, whereas the AP velocity decrease in the BB region was much larger, down to ~0.33 m/s. Slowing of the AP conduction resulted in increasing time delays between APs recorded from the JT and BB regions (see in Fig. 4).

Such a discontinuous conduction is underlain by the AP duration (APD) heterogeneity between the RA and BB cells. As the ADP in the BB cells is relatively long (~250 ms compared to ~170 ms in the RA), the BB region remains relatively refractory at the time when the AP reaches it - as a result, the AP slows down in this region. At the BCL of 200 ms, the AP conduction into the BB region is completely blocked (Fig. 4), as the BB tissue is absolutely refractory. Such AP conduction slowing and blocking in the BB have been observed during experimental rapid pacing of canine atria [19], as well as in patients suffering from AF [17, 20].

IV. DISCUSSION

We have developed a new family of AP models for canine atrial cells (Figs. 1-3), which incorporates experimental data on the ionic channel and AP heterogeneity in dog [8-10, 15]. The single cell models were incorporated into a 1D tissue strand model to simulate the AP conduction and quantify links between the conduction abnormalities and underlying intrinsic heterogeneities in the canine atria (Fig. 4).

Abnormalities in the regions of rapid electrical conduction between the RA and LA - primarily, in the BB - have been associated with delayed activations of the atria and increased incidence of AF [17, 20]. Our simulations demonstrate that the intrinsic APD heterogeneity between the RA and BB cells (Fig. 2) can translate into slowing of the AP conduction velocity in regions with relatively long refractoriness. Such a slowing, and ultimately block, of the AP conduction occurs at rapid pacing rates characteristic of AF (Fig. 4).

Experiments have shown that electrical heterogeneities near the canine PV sleeves can also result in the conduction discontinuities and even re-entrant waves [16, 21]. Our test simulations with a 1D tissue strand comprising of the LA and PV cells demonstrated that the intrinsic APD differences between them (Fig. 3) can result in a conduction block (not shown, similar to Fig. 4). However, studying complex links between electrical heterogeneity and arrhythmic substrates at the PVs is beyond the scope of the present study.

Effects of the intrinsic cellular heterogeneities on the atrial AP conduction have been considered previously [22, 23]. However, interatrial heterogeneities in these studies were not based on relevant electrophysiological data. Ultimately, an efficient computational platform for studying the rapid atrial arrhythmias needs to include both the 3D features of atrial geometry [22, 23] and detailed AP models as developed in our study. Experiments aimed at reconstructing the geometry of the canine atria are in progress in our group. Thus, the next step of our model development will aim to build upon the results of the present study, and include the detailed 3D tissue anatomy into the next generation of atrial models.

Acknowledgments

This work was supported by a project grant from the British Heart Foundation (PG/10/69/28524), United Kingdom.

References

[1]. Anter E, Jessup M, Callans DJ. Atrial fibrillation and heart failure: treatment considerations for a dual epidemic. Circulation. 2009; 119:2516–2525. [PubMed: 19433768]

[2]. Benjamin EJ, Wolf PA, D'Agostino RB, et al. Impact of atrial fibrillation on the risk of death: the Framingham Heart Study. Circulation. 1998; 98:946–952. [PubMed: 9737513]

[3]. Wolf PA, Abbott RD, Kannel WB. Atrial fibrillation as an independent risk factor for stroke: the Framingham Study. Stroke. 1991; 22:983–988. [PubMed: 1866765]

[4]. Harada A, Sasaki K, Fukushima T, et al. Atrial activation during chronic atrial fibrillation in patients with isolated mitral valve disease. Ann. Thorac. Surg. 1996; 61:104–111. [PubMed: 8561533]

[5]. Nattel S, Shiroshita-Takeshita A, Brundel BJ, Rivard L. Mechanisms of atrial fibrillation: lessons from animal models. Prog. Cardiovasc. Dis. 2005; 48:9–28. [PubMed: 16194689]

[6]. Jalife J, Berenfeld O, Mansour M. Mother rotors and fibrillatory conduction: a mechanism of atrial fibrillation. Cardiovasc. Res. 2002; 54:204–16. [PubMed: 12062327]

[7]. Spach MS, Dolber PC, Heidlage JF. Interaction of inhomogeneities of repolarization with anisotropic propagation in dog atria: a mechanism for both preventing and initiating reentry. Circ. Res. 1989; 65:1612–1631. [PubMed: 2582593]

[8]. Li D, Zhang L, Kneller J, Nattel S. Potential ionic mechanism for repolarization differences between canine right and left atrium. Circ. Res. 2001; 88:1168–1175. [PubMed: 11397783]

[9]. Ehrlich JR, Cha TJ, Zhang L, Chartier D, Villeneuve L, Hebert TE, Nattel S. Characterization of a hyperpolarization-activated time-dependent potassium current in canine cardiomyocytes from pulmonary vein myocardial sleeves and left atrium. J. Physiol. 2004; 557:583–597. [PubMed: 15020696]

[10]. Ramirez RJ, Nattel S, Courtemanche M. Mathematical analysis of canine atrial action potentials: rate, regional factors, and electrical remodeling. Am. J. Physiol. 2000; 279:H1767–85.

[11]. Rudy Y. From genome to physiome: integrative models of cardiac excitation. Ann. Biomed. Eng. 2000; 28:945–950. [PubMed: 11144679]

[12]. Aslanidi OV, Boyett MR, Dobrzynski H, Li J, Zhang H. Mechanisms of transition from normal to reentrant electrical activity in a model of rabbit atrial tissue: interaction of tissue heterogeneity and anisotropy. Biophys. J. 2009; 96:798–817. [PubMed: 19186122]

[13]. Aslanidi, OV.; Robinson, R.; Cheverton, D.; Boyett, MR.; Zhang, H. Electrophysiological substrate for a dominant reentrant source during atrial fibrillation. In Conf. Proc. 2009 IEEE Eng. Med. Biol. Soc.; p. 2819-2822.

[14]. Ravelli F, Allessie M. Effects of atrial dilatation on refractory period and vulnerability to atrial fibrillation in the isolated Langendorff-perfused rabbit heart. Circulation. 1997; 96:1686–1695. [PubMed: 9315565]

[15]. Burashnikov A, Mannava S, Antzelevitch C. Transmembrane action potential heterogeneity in the canine isolated arterially perfused right atrium: effect of I_{Kr} and I_{Kur}/I_{to} block. Am. J. Physiol. 2004; 286:H2393–400.

[16]. Chen YJ, Chen SA, Chang MS, Lin CI. Arrhythmogenic activity of cardiac muscle in pulmonary veins of the dog: implication for the genesis of atrial fibrillation. Cardiovasc. Res. 2000; 48:265–273. [PubMed: 11054473]

[17]. O'Donnell D, Bourke JP, Furniss SS. Interatrial transseptal electrical conduction: comparison of patients with atrial fibrillation and normal controls. J. Cardiovasc. Electrophysiol. 2002; 13:1111–1117. [PubMed: 12475102]

[18]. Aslanidi OV, Stewart P, Boyett MR, Zhang H. Optimal velocity and safety of discontinuous conduction through the heterogeneous Purkinje-ventricular junction. Biophys. J. 2009; 97:20–39. [PubMed: 19580741]

[19]. Sakamoto S, Nitta T, Ishii Y, Miyagi Y, Ohmori H, Shimizu K. Interatrial electrical connections: the precise location and preferential conduction. J. Cardiovasc. Electrophysiol. 2005; 16:1077–1186. [PubMed: 16191118]

[20]. Sahadevan J, Ryu K, Peltz L, et al. Epicardial mapping of chronic atrial fibrillation in patients: preliminary observations. Circulation. 2004; 110:3293–3299. [PubMed: 15520305]

[21]. Arora R, Verheule S, Scott L, et al. Arrhythmogenic substrate of the pulmonary veins assessed by high-resolution optical mapping. Circulation. 2003; 107:1816–1821. [PubMed: 12665495]

[22]. Seemann G, Hoper C, Sachse FB, Dossel O, Holden AV, Zhang H. Heterogeneous three-dimensional anatomical and electrophysiological model of human atria. Phil. Trans. Roy. Soc. A. 2006; 364:1465–1481. [PubMed: 16766355]

[23]. Ridler, M.; McQueen, DM.; Peskin, CS.; Vigmond, E. Action potential duration gradient protects the right atrium from fibrillating. Conf. Proc. 2006 IEEE Eng. Med. Biol. Soc.; p. 3978-3981.

Europe PMC Funders Author Manuscripts

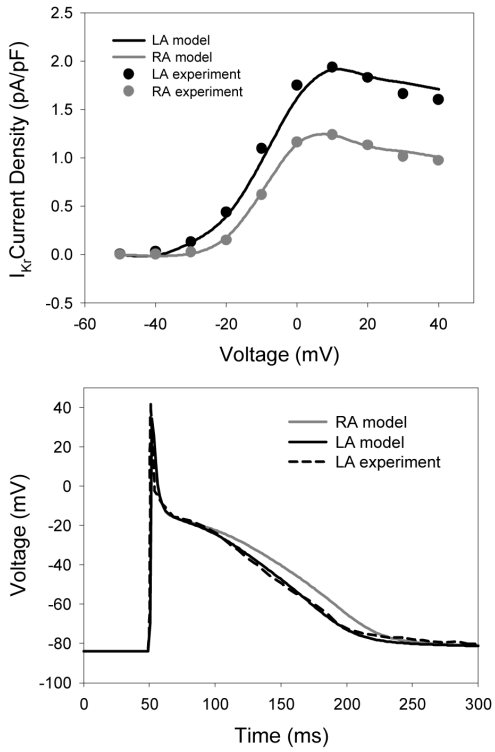

Fig. 1.

Ionic channel and AP heterogeneity between the RA and LA. Top: Differences in the current-voltage relationships for I_{Kr} between the atria. Bottom: Resultant AP differences between the RA and LA models. Model simulations match the experimental recordings [8].

Europe PMC Funders Author Manuscripts

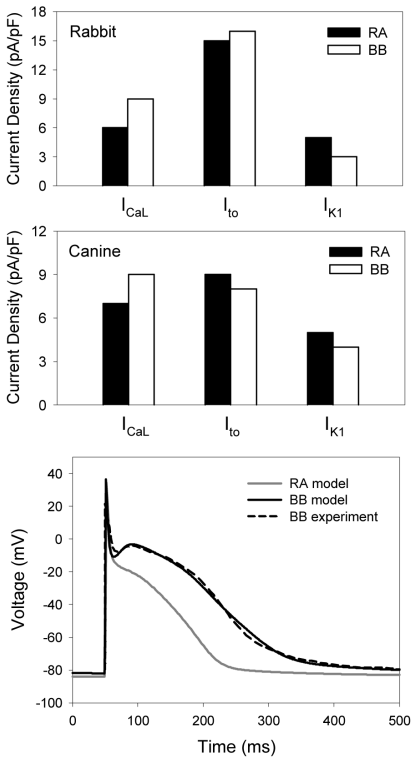

Fig. 2.

Ionic channel and AP heterogeneity between the RA and BB. Top: Differences in the mean ionic current densities between the RA (closed bars) and BB (open bars) in rabbit [13]. Middle: Respective differences introduced between the canine RA and BB cell models. Bottom: Resultant AP differences between the RA and BB models. AP morphology matches the respective experimental recordings [15].

Europe PMC Funders Author Manuscripts

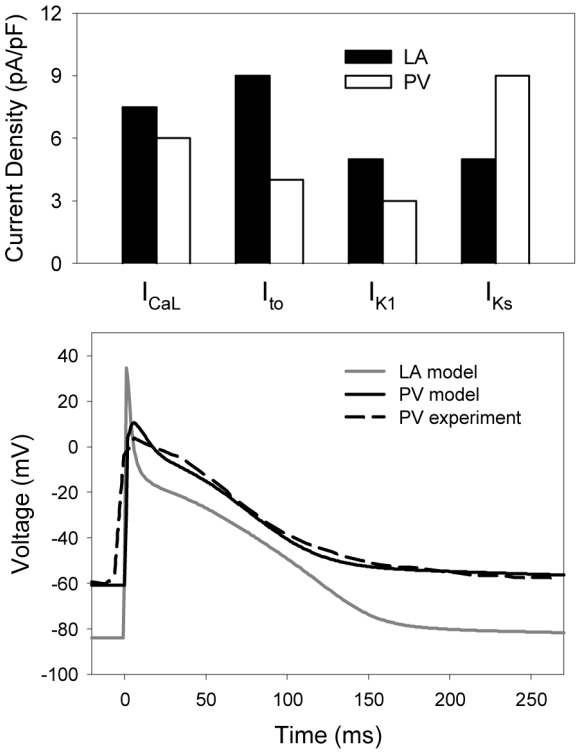

Fig. 3.

Ionic channel and AP heterogeneity between the LA and PV. Top: Differences in the mean ionic channel current densities [9] used between the canine LA (closed bars) and PV (open bars) cell models. Bottom: Resultant AP differences between the LA and PV models.

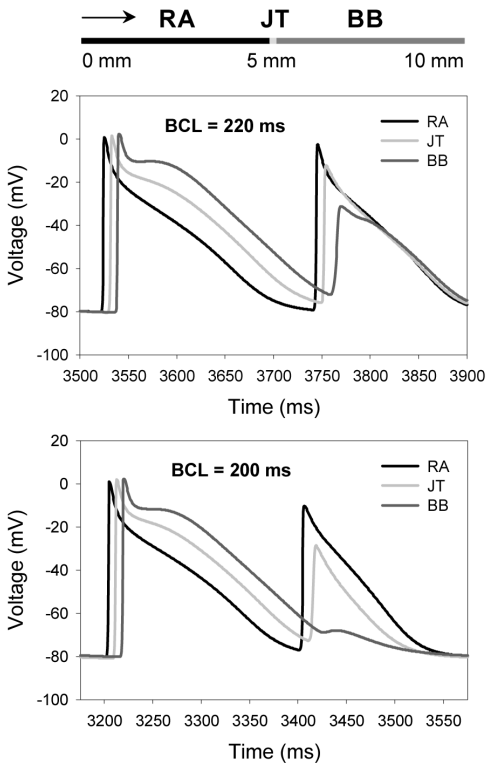

Fig. 4.

Slowing and block of AP conduction between the RA and BB regions of 1D tissue strand. Top: Schematic illustration of the 10 mm strand comprising of the RA cells (0-5 mm) and BB cells (5-10 mm). Arrow shows the direction of AP propagation. APs are recorded from the middle of the RA region, the middle of the BB region and the RA-BB junction (JT). Middle: Slowing of the AP conduction can be seen as the increased time delay between APs from the JT and the BB regions. Bottom: Block of the AP conduction through the BB region.

Europe PMC Funders Author Manuscripts